

## Article

# District Heating for Poorly Insulated Residential Buildings—Comparing Results of Visual Study, Thermography, and Modeling

Stanislav Chicherin <sup>1,2,\*</sup> , Andrey Zhuikov <sup>3</sup>  and Lyazzat Junussova <sup>4</sup>

<sup>1</sup> Thermo and Fluid Dynamics (FLOW), Faculty of Engineering, Vrije Universiteit Brussel (VUB), 1050 Brussels, Belgium

<sup>2</sup> Brussels Institute for Thermal-Fluid Systems and Clean Energy (BRITE), Vrije Universiteit Brussel (VUB) and Université Libre de Bruxelles (ULB), 1050 Brussels, Belgium

<sup>3</sup> Educational and Scientific Laboratory, Siberian Federal University, Krasnoyarsk 660041, Russia

<sup>4</sup> Institute of Heat Power Engineering and Control Systems, Almaty University of Power Engineering and Telecommunications (AUPET), 050013 Almaty, Kazakhstan

\* Correspondence: stanislav.chicherin@vub.be

**Abstract:** Newer buildings have a lower but smoother profile of indoor temperature, while older buildings are less energy efficient. Sometimes, the indoor temperature is unreasonably high, being 25–30 °C. There are buildings where the indoor temperature does not correlate with the outdoor one. Correction factors adjusting convective heat transfer coefficients are suggested. Energy demand is defined using the rate of heat loss and internal heat gains for the given building construction and design consumption profile. We suggest adjusting the setpoints of the secondary supply temperature to keep indoor and return temperatures lower. Correcting a traditional approach when designing a building may minimize energy consumption by 23.3% and increase the annual performance by up to 14.1%. The reductions of thermal peak resulting from a new type of controller adjustment (for instance, discrete) compared to the traditional operation range from roughly 10 to 30%, respectively. A better understanding of the system operation is a necessary step to switch to fourth-generation district heating (4GDH). This methodology is especially helpful in shaving daily peaks of heat demand. Building envelopes ease the charging, maximum storage capacity, and balance of the given generation and demand profiles, which are key factors in achieving the reduction in greenhouse gas (GHG) emissions. Once the heat demand is covered according to the maximum storage capacity for the given generation and demand profile, fewer efforts to modernize a district heating network are required.

**Keywords:** energy; building; demand; window; envelope; supply



**Citation:** Chicherin, S.; Zhuikov, A.; Junussova, L. District Heating for Poorly Insulated Residential Buildings—Comparing Results of Visual Study, Thermography, and Modeling. *Sustainability* **2023**, *15*, 14908. <https://doi.org/10.3390/su152014908>

Academic Editors: Higinio Sánchez-Sáinz and Raúl Sarrias-Mena

Received: 21 September 2023

Revised: 8 October 2023

Accepted: 10 October 2023

Published: 16 October 2023



**Copyright:** © 2023 by the authors. Licensee MDPI, Basel, Switzerland. This article is an open access article distributed under the terms and conditions of the Creative Commons Attribution (CC BY) license (<https://creativecommons.org/licenses/by/4.0/>).

## 1. Introduction

Excluding demand-side measures, there are other ways of suggesting optimal strategies for the management of district heating (DH) systems. In [1], both temperature boosting and thermal energy storage are considered. The capacity of a typical short-term energy storage of a hot water buffer tank is usually up to 50 MWh. In [2], the sum of the energy absorbed by the distribution system, the district heating (DH) substations, space heating (SH) systems, and radiators, and the energy released by the sensible heat accumulator are 10 times higher—330 and 440 MWh, respectively.

In [3], the system is preheated well before the outdoor temperature is expected to decrease below the design outdoor temperature (DOT). This results in continuous transient processes and is associated with errors, meaning the DH network should not be ignored as a thermal accumulator. Therefore, our novelty is that we begin our research from the study of operational profiles on a primary side of the DH system; these operational profiles have already taken all the transient processes into account. Some methodologies are able to detect peaks happening due to the transient behavior [4] or internal heat gains [5].

In [6], an office building is modeled and simulated in TRNSYS, inputting the solar radiation and weather data from the local meteorological station. In the heat supply, flexibility is typically created by temporarily increasing the supply temperature [7]. Sun et al. [8] report an indoor temperature deviation of 1 °C, while the correction range of a substation supplying a radiator with no TRV is the largest, about 4 °C. They even impose an upper threshold of adjustment and set it to 5 °C to ensure the stable operation of the DH system. Similar equations and plots, as shown in [9] are used here to assess the daily fluctuation of supply and indoor temperatures. Furthermore, Sleptsov et al. [10] compared these controllers' performance to find out the perspectives of suggested controllers in contemporary HVAC systems. The limitations of most of the control patterns are that they only utilize setbacks (especially daily ones) to a very limited extent. On the other hand, there are a lot of research attempts devoted to the wider use of operational data. For instance, Ivanko et al.'s paper [11] again. They present the recorded SH and DHW consumption profiles before and after the control point temperature is achieved to make the control point temperature be recognized by visual analysis and the regression methods. For the described case study, the structuration aids (control logic and transformation measure prioritization) and the numeric values (temperature and pressure) describe the operational strategy. It is generalized enough to be highly practical and being presented in this form, it provides a good overview of the input and output data and its visualization. Previously, the authors focused on the available technologies mainly applicable to a heat pump [12], of which utilization showed that the energy-saving effect might be significantly improved but did not deal with raw operational data on electricity and gas demands. Saletti et al. [13] consider not only simulation results but also operational data derived from the substation heat exchanger of the Skultuna buildings. It is a locality situated in Västerås Municipality, Västmanland County, Sweden with 3133 inhabitants. They compare it to the design values and apply operational data as a setpoint for the optimization. Braas et al. [14] present normalized duration curves of energy consumption, i.e., the heat demand in each time step of the year, divided by the peak load of the respective load profile. Unlike us, they study buildings with and without thermal energy storage but focus on the duration curve of a single building, comparing it with the duration charts for 100 superposed buildings of the same type. Another difference is the emphasis on residential buildings and synthesizing the heat demand profile for each of them, not with the same but with statistically varied DHW draw-off profiles [15].

The prosumer is the consumer, which may also produce heat; it could be an office building and a hospital, or a typical mixed-use district comprising also residential buildings [16]. Unlike us, Sommer et al. [16] input pre-set hourly energy consumption profiles for space heating SH, domestic hot water DHW, and space cooling for each prosumer. These demands are covered by the heat pumps HPs and heat exchangers in the prosumers. If the primary supply temperature is relatively low, its level at the demand side can be boosted with the help of a heat pump (HP), using the heat distribution network as a heat source. However, this will increase electricity consumption from a power grid or require installing additional equipment, e.g., heat pumps.

Kauko et al. [17] used Dymola for simulations, which stands for Dynamic Modeling Laboratory. It is a dynamic simulation tool, based on the object-oriented modeling language Modelica. Although the object-oriented approach implies an equation-based modeling language, it requires declaring relations among every variable within a class of a procedure. Moreover, its re-usability, as well as the extensibility and adaptability of the created models, is limited in case any other parts are developed in other languages, e.g., in Python. In [18], the model is developed in Modelica as well, but with the help of the models from the AixLiblibrary, while the Python tool uesgraphs is used to input the network data. Unlike us, energy production and consumption models are adapted primarily for interaction with the MPC and are established with the help of a traditional degree-day approach. In [19], NetSim software is applied. Each scenario is simulated for 10 temperature intervals ranging between −18 and +30 °C. These temperatures are the average ones of each temperature

interval. In addition, simulations in NetSim are static. Compared to these papers, we use Python, study many more factors than just outdoor temperature, do not use such an artificial categorization, and do not use commercial software (e.g., NetSim).

Another limitation is reasoned to the specific features of a DH system. For the DH case, a reference group-based approach cannot be directly used by the individual substations to run any sort of automatic control mechanism when a problem is detected. Substations are also operated not obligatorily smoothly, but sometimes in a discrete manner, which makes energy consumption also discrete in its distribution throughout the year or even a day. Such behavior is reasoned to the very nature of PI and PID controllers and temperature setpoints. To adjust to the change in energy consumption, Chertkov et al. [20] vary the temperature setpoints during the day. In their model, it generates a heat wave moving with the speed of the mass flow, which is also different. It might be a tenth of a meter or a few meters per second depending on the scale of a DH system. The difference is their attention to only one factor of energy distribution, which is also mostly true for large DH systems only. They study the transient behavior and the delay, which takes minutes to hours and depends on the location of a consumer. It also does not necessarily reflect any correlation, because heat demand depends not only on the time of day but also on the type of day (weekend or weekday) and season.

To compare, Farouq et al. [21] detected more random behavior compared to its reference group, comprised mostly of residential buildings, and reasoned it to a malfunction or inadequate setpoints for some control parameters at the target regulators. Synthetic heat demand profiles are also useful for removing clearly visible errors—indistinct measurements or apparently incorrect readings (utterly high or low values) [22].

Siuta-Olcha et al. [23] highlight the importance of operational data and discuss it in comparison to actual heat consumption before and after the modernization of DH area substations in Warsaw (Poland) from 1999 to 2002.

A deep reinforcement learning agent based on adaptive variables was compared with an agent trained with more classic non-adaptive variables. The comparison was performed by modeling the deployment of the two agents in four different scenarios. The issue is that they all deal with theoretical inputs and assumptions such as DOT, the control point temperature, the indoor temperature setpoint, and the constant occupancy schedule. Our contribution to the pool of knowledge is an emphasis on operational data and results from visual and technical inspections of existing buildings.

Another work about energy transfer stations and operational data is [24]. However, the aim of Jangsten et al.'s [24] paper is to reveal reasons for high return temperature and suggest potential solutions, augmented with an attempt to increase the knowledge about the operation of DH substations.

To compare objects of a case study, analyzing Luc et al.'s [25] and Harney et al.'s [26] papers was worthwhile. Luc et al. [25] study a new office building and conclude that there is some period when the internal heat gains may alleviate the reduction in indoor temperature. Unlike that study, Ivanko et al. [11] studied the SH heat use in a hotel and concluded it to be different from the typical theoretical assumption. Harney et al. [26] draw attention to residential buildings. A flat detailed in their paper belongs to the reference dwelling described by the Irish Department of Housing, Planning, and Local Government, as part of the public hearing for novel, tightened legislation on construction in Ireland.

The size of an accumulator is currently defined by analyzing the profiles for heat generation and demand. Excessive generation is evaluated by assuming all the surplus heat to be dumped into the building envelopes and all the difference to be covered by an accumulator. However, this is not correct because infiltration and internal heat gains are highly variable, not to mention the appliance of this method is limited at the design stage since there is no operational data. Hence, the obtained results are representative and principal since the model addresses these challenges and supports cutting off these peaks. The novelty is in defining excessive generation as the point where the energy generated exceeds the sum of the heat consumed and energy losses considering the heat gains.

Since the demand-side phenomena become increasingly crucial, the energy performance of the building envelope increases with every year of construction. To make our paper clear in the description of the scientific novelty, in comparison to what has previously been published in the literature on the same topic, the methodology is compared to the closest papers—Sun et al. [8], Ren et al. [27], and Camci et al. [28].

## 2. Materials and Methods

$Q_{in}$  heat gain [W] (Adopted from SP 50.13330.2012 Thermal protection of buildings Sc. and research institute of the construction physics of RAASN, Moscow, 2018),

$$Q_{in} = q_{in} \cdot A_{in}, \quad (1)$$

where  $A_{in}$  is an indoor area [ $m^2$ ],  $q_{in}$  is the specific heat gain according to the list of gadgets, machines, and equipment [ $W/m^2$ ]; for residential buildings, empirical formulae might be applied <sup>1</sup>

$$q_{in} = 17 - (A_{in}/N - 20) \cdot 7/25, \quad (2)$$

where  $N$  is the number of inhabitants.

The amount of heat released from radiators to keep infiltrating air warm is [W], <sup>1</sup>

$$Q_{inf} = 0.28 \cdot G_{inf} \cdot c_a \cdot A \cdot (t_{in} - t_{out}^d) \cdot k, \quad (3)$$

where  $G_{inf}$  is the amount of air infiltrating [ $kg/(hm^2)$ ],  $c_a$  is the specific heat capacity of air;  $c_a = 1.006 \text{ kJ}/(kg \cdot ^\circ C)$ ,  $k$  is the adjusting factor, set to:

- 0.7 for triple-glazed doors (both main and emergency) and windows.
- 0.8 for double-glazed doors (both main and emergency) and windows.
- 1 for other doors (both main and emergency) and windows.

The amount of air infiltrating [ $kg/(hm^2)$ ] is as follows: <sup>1</sup>

- for windows,

$$G_{inf} = (1/R_{inf,wind}) \cdot (\Delta P / \Delta P_o)^{2/3}, \quad (4)$$

- for doors,

$$G_{inf} = (1/R_{inf,door}) \cdot (\Delta P / \Delta P_o)^{1/2}, \quad (5)$$

where  $R_{inf,wind}$  is the specific infiltration rate of a window for a design pressure difference of 10 Pa [ $hm^2/kg$ ], typically input according to the manufacturer's information,  $R_{inf,door}$  is the specific infiltration rate of a door (both main and emergency) [ $hm^2/kg$ ], set to:

- 0.85 for triple doors and two airlocks between and for double doors, if an air door (curtain) is installed <sup>1</sup>,
- 0.7 for double doors and one airlock between <sup>1</sup>,
- 0.47 for residential buildings and revolving doors, if an air door (curtain) is installed <sup>1</sup>,
- 0.16 for four-wing revolving door <sup>1</sup>,
- 0.14 for three-wing revolving doors <sup>1</sup>,
- 0.07 for a single (incl. balcony) door <sup>1</sup>.

$\Delta P$  is the pressure difference for a specific location and terrain [Pa];

$\Delta P_o$  is the design pressure difference, set to 10 Pa.

To ensure a more accurate assessment of energy consumption, a method should be able to predict the heat demand affected by air pressure distribution, <sup>1</sup>

$$Q_{vent} = 0.28 \cdot L_{vent} \cdot \rho_{in} \cdot c_a \cdot (t_{in} - t_{out}^d), \quad (6)$$

where  $L_{vent}$  is the ventilation flow rate [ $m^3/h$ ],  $\rho_{in}$  is the specific air density of indoor air [ $kg/m^3$ ].

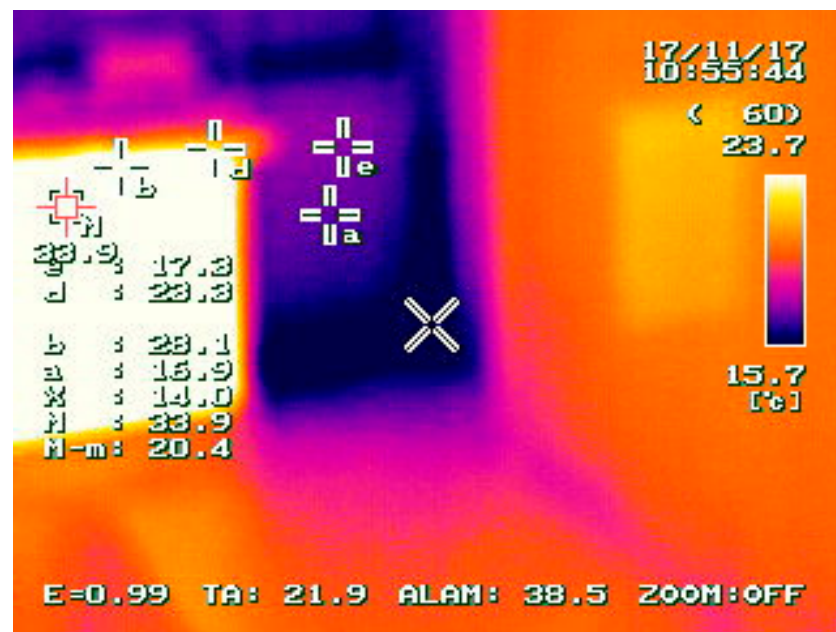
The temperature of air coming out of a vent [°C] is typically defined as <sup>1</sup>

$$t_{com} = t_{in} + (Q_{env} - Q_{in}) / (L_{vent} \cdot \rho_{in} \cdot c_a). \quad (7)$$

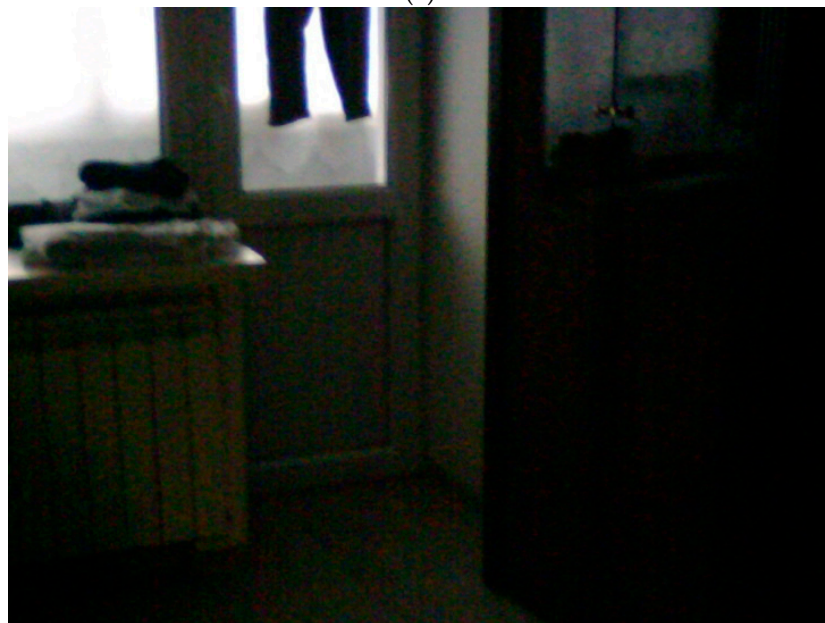
All the calculations of heat demand and temperature profiles were performed by Temper-3d© (6.14.01, Russia, Omsk) software.

### 3. Results and Discussion

Figure 1 indicates the temperature profiles of window and balcony doors resulting in additional heat consumption during the coldest period of the year.



(a)



(b)

Figure 1. Cont.

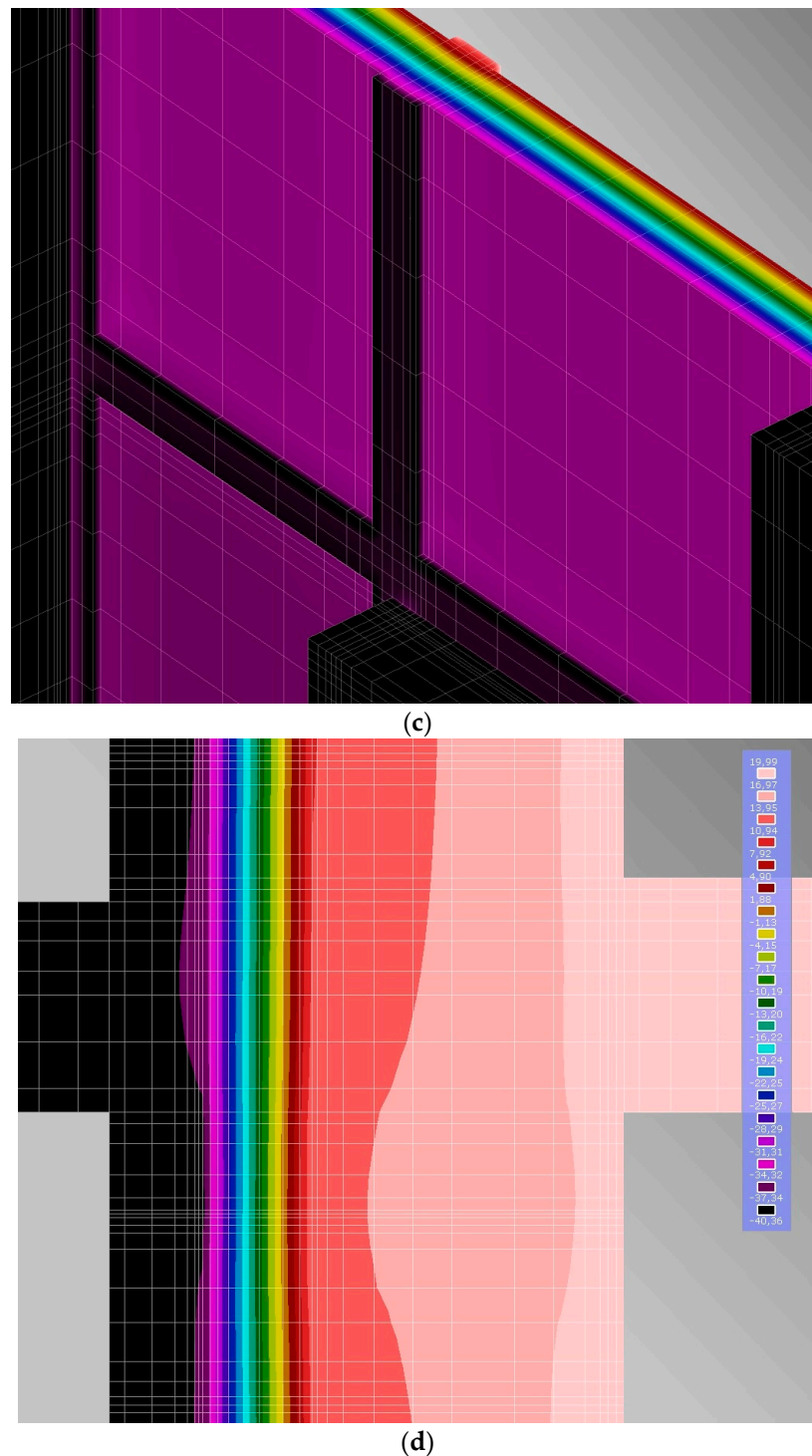
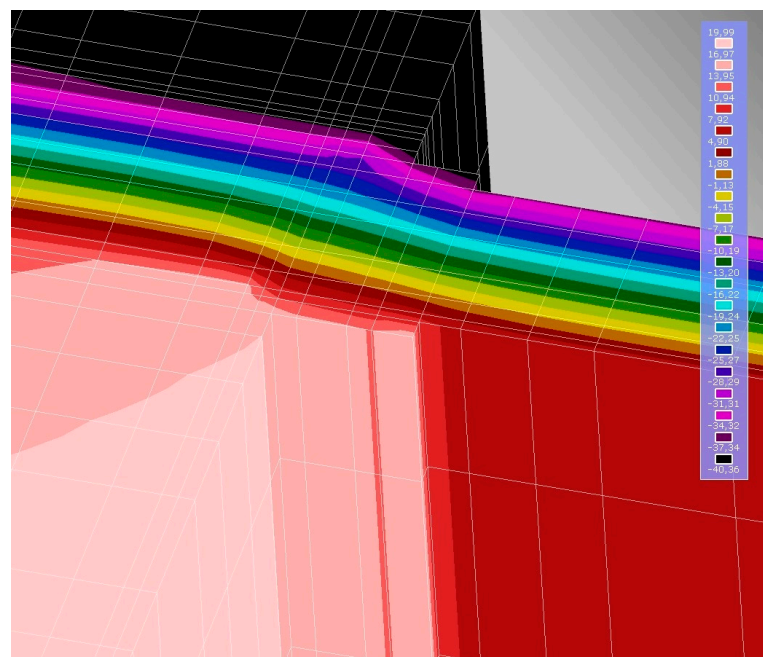


**Figure 1.** Temperature profiles and visual imagery: (a,b) actual, (c) modeled as traditional. The temperature profiles are even and smooth and all the borders between temperature zones are represented by straight lines; (d) simulated setting of actual temperatures as boundary conditions and applying  $\beta$ -factor for a door.

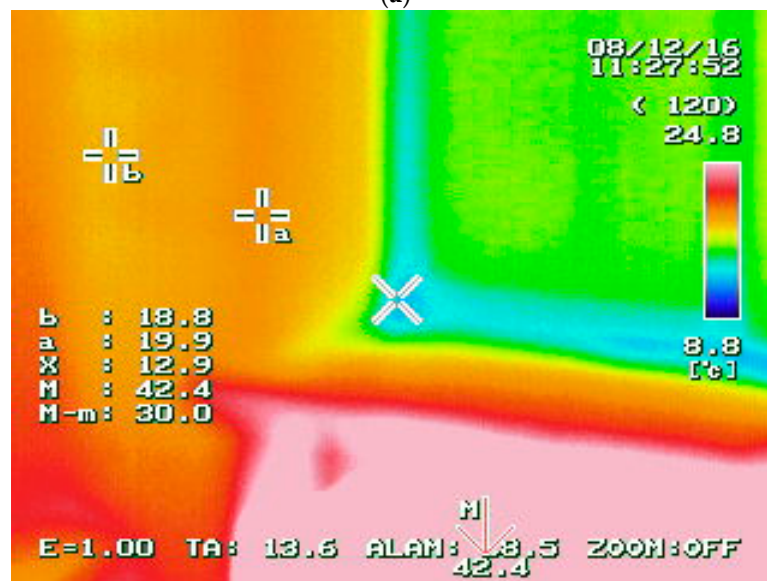
For the same boundary conditions and the same structural construction, Figure 1 shows the distribution of indoor temperature according to the novel methodology that also includes an increased heat demand compared to the reference scenario. Around 10% of heat (excessive amount of energy above the design threshold) is lost according to this calculation. In the case of an old building used for commercial purposes, it is covered by

an even higher heat demand increase (up to 20%) between 7 a.m. and 5 p.m. Otherwise, the drop in indoor temperature is expected at 17:00, which corresponds to the reduction in internal heat gains in office buildings and the same energy consumption at that time. Secondly, the approach based on adjusted variables ( $R_{inf,door}$  and  $k$ ) was only able to indicate the variation of temperature fields closer to the thermography. Temper software also adapts to the change in indoor temperature requirements, maintaining more accurate boundary conditions within the zone, despite any learning that goes on during static deployment. For instance, Figure 1d shows the surface temperature of 19.9 °C rather than 4.9 °C in Figure 1c.

The next step of the methodology is to study the edges of the wall and ceiling with different temperatures, as displayed in Figure 2.

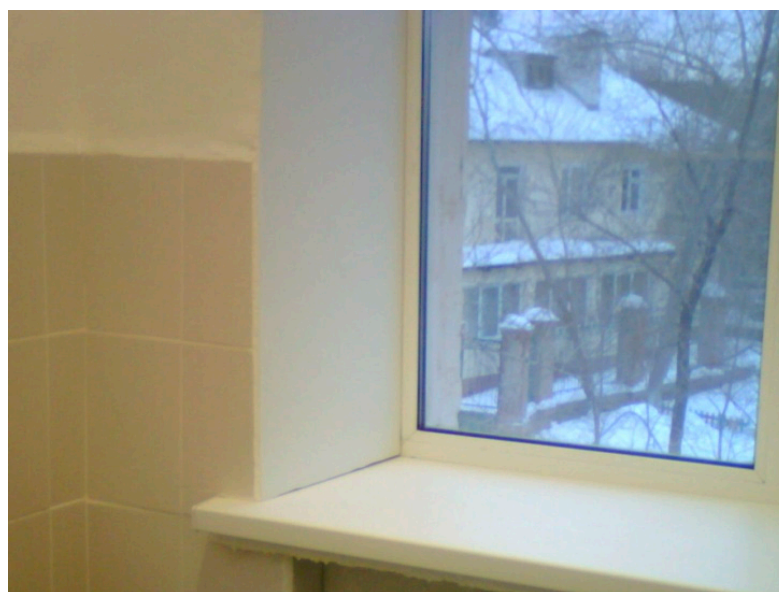


(a)



(b)

Figure 2. Cont.



(c)

**Figure 2.** Contours of temperature (a) compared to actual temperatures (b) obtained from the Temper-3d© simulation and linear temperature model applied to a typical window (c).

To enhance the thermal performance of worn-out structures and consequently decrease energy consumption, the integration of the actual temperature distribution of inner surface wallboards or furniture elements is a promising decision. In the present research, taking the contents of the apartment into account may increase the U-factor by 1.56 and 1.17 times in the cases of low-insulation and high-insulation light-structure houses, respectively.

As mentioned above, the performance of the envelopes is the key factor defining the heat demand of a building. When  $R$  is fixed at 3.15 or 0.54  $\text{m}^2 \text{ }^\circ\text{C}/\text{W}$  with  $\beta$  set to 0.1 or 0.05, the effected heat consumption is up to 444 W, which is purely according to the characteristics described in Figure 2. The average error is found then to be in the range of 5%, with some values above, indicating that the suggested methodology is more correct when assessing heat demand. In response to the increasing factors of insolation and internal heat gains to 51  $\text{W}/\text{m}^3$  and 68  $\text{W}/\text{m}^3$ , respectively, the prediction errors for the linear temperature model increase. Correcting a traditional approach when designing a building may minimize the peak energy consumption by 23.3% and increase the annual performance by up to 14.1%.

To compare, Ren et al. [27] assume a specific heat transfer of 34  $\text{W}/\text{m}^3$  with a U-value below 0.063; the maximum error is then 20%, which is much lower compared to those presented here. This results in a 5% or less discrepancy, indicating that their model has a low error when forecasting indoor temperature. According to Johra et al. [29], furniture with advanced analysis could increase the heat demand by up to 87 and 30% in the cases of low-insulation and high-insulation light-structure houses, respectively. Ren et al. [27] conclude when setting heat transfer to 51 and 68  $\text{W}/\text{m}^3$ , the prediction errors for a linear model increase.

Table 1 indicates that the heat demand is much lower before adopting factors for thermal inertia, and the variation is also large for different offices, with a total difference of 6952.6 and an average of 54.7 W.

**Table 1.** The adjustment factors and heat consumption corresponding to different zones. There is one main entrance and several emergency exits on the ground- and first floors, in addition to fire escapes on the second, third, and fourth floors. Walls adjacent to the indoor spaces with colder design indoor temperature (e.g., a staircase or a vestibule) contributing to overall heat losses are titled ‘internal partitions’.

#	Office (Zone)	Target Indoor Temperature [°C]	Properties of Envelopes		R-Value [m <sup>2</sup> K/W]	$t_{in}^d - t_{out}^d$	Design Heat Demand [W]	Corrections			Adjusted Heat Demand [W]	Total Heat Demand [W]
			Wall Title (According to the Blueprints)	Orientation				Adjustment Factor $\beta$	Adjustment Factor $k$	Overall Correction (1 + $\Sigma\beta$ )		
1	Tool shop	16	Internal partition #1		2.1	53	2862	0	n/a	1.0	2862	6325
		16	Internal partition #2		4.3	53	1361	0	n/a	1.0	1361	
		16	Internal partition #3		8.6	53	724	0	n/a	1.0	724	
		16	Internal partition #4		14.2	53	676	0	n/a	1.0	676	
		16	Window	NE	0.54	53	424	0.1	0.8	1.1	466.6	
		16	Door	SW	0.54	53	235	0	1	1.0	235	
2	Storage room for household chemical goods. garage	16	Internal partition #1		2.1	53	3408	0	n/a	1.0	3408	7835
		16	Internal partition #2		4.3	53	1935	0	n/a	1.0	1935	
		16	Internal partition #3		8.6	53	876	0	n/a	1.0	876	
		16	Internal partition #4		14.2	53	814	0	n/a	1.0	814	
		16	Window	NE	0.54	53	494	0.1	0.8	1.1	544	
		16	Door	NW	0.54	53	235	0.1	1	1.1	258	
13	Office	20	Load-bearing wall	SW	3.15	57	235	0	n/a	1.0	235	708
		20	Load-bearing wall	NW	3.15	57	430	0.1	n/a	1.1	473	

Table 1. Cont.

#	Office (Zone)	Target Indoor Temperature [°C]	Properties of Envelopes		R-Value [m <sup>2</sup> K/W]	$t_{in}^d - t_{out}^d$	Design Heat Demand [W]	Corrections			Adjusted Heat Demand [W]	Total Heat Demand [W]
			Wall Title (According to the Blueprints)	Orientation				Adjustment Factor $\beta$	Adjustment Factor $k$	Overall Correction (1 + $\Sigma\beta$ )		
12	Exhibition hall	20	Load-bearing wall	SW	3.15	57	860	0	n/a	1.0	860	8569
		20	Window	SW	0.54	57	912	−0.1	0.8	0.9	821	
		20	Window	SW	0.54	57	912	−0.1	0.8	0.9	821	
		20	Load-bearing wall	SE	3.15	57	664	−0.05	n/a	0.95	632	
		20	Window	SE	0.54	57	1158	−0.05	0.8	0.95	1103	
		20	Load-bearing wall	NW	3.15	57	704	0.1	n/a	1.1	774	
		20	Door	NE	0.54	57	456	0.1	1	1.1	502	
		20	Load-bearing wall	NE	3.15	57	521	0.1	n/a	1.1	573	
		20	Window	NE	0.54	57	336	0.1	0.8	1.1	370	
		20	Load-bearing wall	NE	3.15	57	391	0.1	n/a	1.1	430	
		20	Door	NW	0.54	57	456	0.1	1	1.1	502	
		20	Window	SW	0.54	57	912	−0.1	0.8	0.9	821	
	Staircase/ Vestibule	16	Load-bearing wall	SW	3.15	53	182	−0.1	n/a	0.9	164	1102
		16	Load-bearing wall	NW	3.15	53	448	0.1	n/a	1.1	493	
		16	Load-bearing wall	NE	3.15	53	182	0.1 + 0.27 × 3.6	n/a	2.072	377	
		16	Door	NE	0.54	53	206	0.1	1	1.1	227	
2	Vestibule	20	Load-bearing wall	SW	3.15	57	278	0	n/a	1.0	278	936
		20	Door	SW	0.54	57	329	−0.1	1	0.9	296	
		20	Door	SW	0.54	57	329	−0.1	1	0.9	296	

Table 1. Cont.

#	Office (Zone)	Target Indoor Temperature [°C]	Properties of Envelopes		R-Value [m <sup>2</sup> K/W]	$t_{in}^d - t_{out}^d$	Design Heat Demand [W]	Corrections			Adjusted Heat Demand [W]	Total Heat Demand [W]
			Wall Title (According to the Blueprints)	Orientation				Adjustment Factor $\beta$	Adjustment Factor $k$	Overall Correction (1 + $\Sigma\beta$ )		
3	Office	20	Window	NE	0.54	57	1900	0.1	0.8	1.1	2090	4720
		20	Window	SE	0.54	57	1900	−0.05	0.8	0.95	1805	
		20	Internal partition #1		2.1	57	543	0	n/a	1.0	543	
		20	Internal partition #2		4.3	57	90	0	n/a	1.0	90	
		20	Internal partition #3		8.6	57	2	0	n/a	1.0	2	
	Staircase	16	Load-bearing wall	NW	3.15	57	418	0.1	n/a	1.1	460	1334
		16	Load-bearing wall	NE	3.15	57	300	0.1	n/a	1.1	330	
		16	Load-bearing wall	SW	3.15	57	300	0	n/a	1.0	300	
		16	Door	NW	0.54	57	222	0.1	1	1.1	244	
4	Exhibition hall	20	Load-bearing wall	NW	3.15	57	391	0.1	n/a	1.1	430	17,294
		20	Load-bearing wall	SW	3.15	57	521	0	n/a	1.0	521	
		20	Window	SW	0.54	57	897	0	0.8	1.0	897	
		20	Window	SE	0.54	57	7600	0.05	0.8	1.05	7980	
		20	Load-bearing wall	NE	3.15	57	1368	0.1	n/a	1.1	1505	
		20	Door	NE	0.54	57	329	0.1	1	1.1	362	
		20	Window	NE	0.54	57	1368	0.1	0.8	1.1	1505	
		20	Load-bearing wall	NW	3.15	57	782	0.1	n/a	1.1	860	
		20	Window	NW	0.54	57	684	0.1	0.8	1.1	752	
		20	Door	NW	0.54	57	456	0.1	1	1.1	502	
		20	Internal partition #1		2.1	57	1357	0	n/a	1.0	1357	
		20	Internal partition #2		4.3	57	504	0	n/a	1.0	504	
20	Internal partition #3		8.6	57	119	0	n/a	1.0	119			

Table 1. Cont.

#	Office (Zone)	Target Indoor Temperature [°C]	Properties of Envelopes		R-Value [m <sup>2</sup> K/W]	$t_{in}^d - t_{out}^d$	Design Heat Demand [W]	Corrections			Adjusted Heat Demand [W]	Total Heat Demand [W]
			Wall Title (According to the Blueprints)	Orientation				Adjustment Factor $\beta$	Adjustment Factor $k$	Overall Correction (1 + $\Sigma\beta$ )		
12	Office	20	Window	SW	0.54	57	8312	0	0.8	1.0	8312	16,822
		20	Window	NW	0.54	57	3958	0.1	0.8	1.1	4354	
		20	Window	SE	0.54	57	3958	0.05	0.8	1.05	4156	
	Staircase	16	Load-bearing wall	NE	3.15	53	379	0.1	n/a	1.1	417	1955
		16	Window	NE	0.54	53	368	0.1	0.8	1.1	405	
		16	Load-bearing wall	SW	3.15	53	561	0.05	n/a	1.05	589	
		16	Load-bearing wall	NW	3.15	53	126	0.1	n/a	1.1	139	
		16	Window	NW	0.54	53	368	0.1	0.8	1.1	405	
		20	Load-bearing wall	NW	3.15	57	426	0.1	n/a	1.1	469	
6	Hallway	20	Door	NW	0.54	57	259	0.1	1	1.1	285	2001
		20	Load-bearing wall	NW	3.15	57	122	0.1	n/a	1.1	134	
		20	Load-bearing wall	NW	3.15	57	122	0.1	n/a	1.1	134	
		20	Load-bearing wall	NE	3.15	57	277	0.1	n/a	1.1	305	
		20	Window	NE	0.54	57	285	0.1	0.8	1.1	314	
		20	Load-bearing wall	SE	3.15	57	144	0.05	n/a	1.05	151	
		20	Window	NW	0.54	57	190	0.1	0.8	1.1	209	
		20	Window	NW	0.54	57	190	0.1	0.8	1.1	209	
11	Office	20	Window	SW	0.54	57	2375	0	0.8	1.0	2375	2375
19	Office	20	Load-bearing wall	NE	3.15	57	271	0.1	n/a	1.1	298	1164
		20	Window	NE	0.54	57	190	0.1	0.8	1.1	209	
		20	Load-bearing wall	NW	3.15	57	407	0.1	n/a	1.1	448	
		20	Window	NW	0.54	57	190	0.1	0.8	1.1	209	
1	Office	20	Load-bearing wall	NW	3.15	57	407	0.1	n/a	1.1	448	657
		20	Window	NW	0.54	57	190	0.1	0.8	1.1	209	

Table 1. Cont.

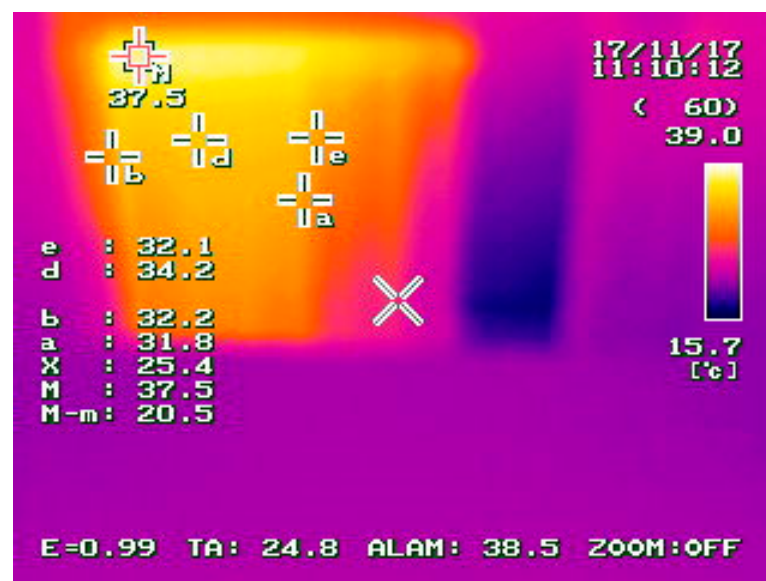
#	Office (Zone)	Target Indoor Temperature [°C]	Properties of Envelopes		R-Value [m <sup>2</sup> K/W]	$t_{in}^d - t_{out}^d$	Design Heat Demand [W]	Corrections			Adjusted Heat Demand [W]	Total Heat Demand [W]
			Wall Title (According to the Blueprints)	Orientation				Adjustment Factor $\beta$	Adjustment Factor $k$	Overall Correction (1 + $\Sigma\beta$ )		
2.3	Office	20	Load-bearing wall	NE	3.15	57	814	0.1	n/a	1.1	895	1731
		20	Window	NE	0.54	57	760	0.1	0.8	1.1	836	
4	Office	20	Load-bearing wall	NE	3.15	57	339	0.1	n/a	1.1	373	2224
		20	Load-bearing wall	NE	3.15	57	611	0.1	n/a	1.1	672	
		20	Load-bearing wall	SE	3.15	57	407	0.05	n/a	1.05	427	
		20	Window	NE	0.54	57	684	0.1	0.8	1.1	752	
		20	Window	SE	0.54	57	2375	0.05	0.8	1.05	2494	
10	Office	20	Window	SE	0.54	57	4750	0.05	0.8	1.05	4988	8155
20	Window	SW	0.54	57	3167	0	0.8	1.0	3167			
14	Office	20	Load-bearing wall	NW	3.15	57	407	0.1	n/a	1.1	448	646
		20	Window	NW	0.54	57	180	0.1	0.8	1.1	198	
20	Office	20	Load-bearing wall	NW	3.15	57	407	0.1	n/a	1.1	448	3976
		20	Load-bearing wall	SW	3.15	57	204	0	n/a	1.0	204	
		20	Window	NW	0.54	57	1583	0.1	0.8	1.1	1741	
		20	Window	SW	0.54	57	1583	0	0.8	1.0	1583	
		20	Window	NW	0.54	57	3132	0.1	0.8	1.1	3445	
14	Office	20	Window	SW	0.54	57	3132	0	0.8	1.0	3132	12,754
		20	Window	SE	0.54	57	3569	0.05	0.8	1.05	3748	
		20	Window	NE	0.54	57	1821	0.1	0.8	1.1	2003	
		20	Internal partition		4.18	57	426	0	n/a	1.0	426	
		20	Window	NE	0.54	57	2404	0.1	0.8	1.1	2644	
5	Office	20	Window	NW	0.54	57	3205	0.1	0.8	1.1	3526	6341
		20	Door	NW	0.54	57	155	0.1	1	1.1	171	

Table 1. Cont.

#	Office (Zone)	Target Indoor Temperature [°C]	Properties of Envelopes		R-Value [m <sup>2</sup> K/W]	$t_{in}^d - t_{out}^d$	Design Heat Demand [W]	Corrections			Adjusted Heat Demand [W]	Total Heat Demand [W]
			Wall Title (According to the Blueprints)	Orientation				Adjustment Factor $\beta$	Adjustment Factor $k$	Overall Correction (1 + $\Sigma\beta$ )		
1	Security room	20	Window	NW	0.54	57	874	0.1	0.8	1.1	961	961
13	Hallway	20	Window	NW	0.54	57	947	0.1	0.8	1.1	1042	1376
		20	Door	SE	0.54	57	222	0.05	1	1.05	233	
		20	Window	SW	0.54	57	101	0	0.8	1.0	101	
9	Lounge	20	Window	SE	0.54	57	3350	0.05	0.8	1.05	3518	4975
		20	Window	SW	0.54	57	1457	0	0.8	1.0	1457	
6	Exhibition hall	20	Window	NE	0.54	57	4443	0.1	0.8	1.1	4887	6990
		20	Window	SE	0.54	57	2003	0.05	0.8	1.05	2103	
	Vestibule	20	Window	SW	0.54	57	2185	0	0.8	1.0	2185	2185
7	Vestibule	18	Window	SE	0.54	55	422	0	0.8	1.0	422	422
3	Vestibule	18	Window	NW	0.54	55	351	0.1	0.8	1.1	386	386
15	Vestibule	18	Window	SW	0.54	55	351	0	0.8	1.0	351	351
2	Principal's office	20	Window	SW	0.54	57	1710	0	0.8	1.0	1710	4569
		20	Internal partition		4.18	57	246	0	n/a	1.0	246	
		20	Window	NW	0.54	57	2375	0.1	0.8	1.1	2613	
1	Reception	20	Internal partition		4.18	57	246	0	n/a	1.0	246	4565
		20	Window	NE	0.54	57	1786	0.1	0.8	1.1	1965	
		20	Window	IOB	0.54	57	2242	0.05	0.8	1.05	2354	
4	Bathroom	20	Window	NE	0.54	57	456	0.1	0.8	1.1	502	502
3	Lounge area	20	Window	NE	0.54	57	1425	0.1	0.8	1.1	1568	2509
		20	Window	NW	0.54	57	855	0.1	0.8	1.1	941	

When assessing a big mall, an office building, or an ice-skating rink with multiple doors, the difference is expected to be much larger. After adopting the suggested methodology, the standard deviation is 1404.1 W, the variation amplitude for each space is small, with a maximum value of 2.072, a minimum value of 1.05, and an average of 1.07. Thus, compared with the traditional approach, the new one may ensure better indoor comfort. At the same time, it decreases energy consumption for the operation of the DH network. Currently, the heat demands of the closest rooms to the windows oriented to the south do not result in 26 °C, while the heat demands of the other spaces are still mostly affected by the internal heat gains due to the consumers' behavior (previously obtained when the consumption was still detected).

Therefore, an additional study at a residential building has been performed to quantify the contribution of the faulty components of a SH system or additional heaters in the creation of the peaks of return temperature; the results are shown in Figure 3.

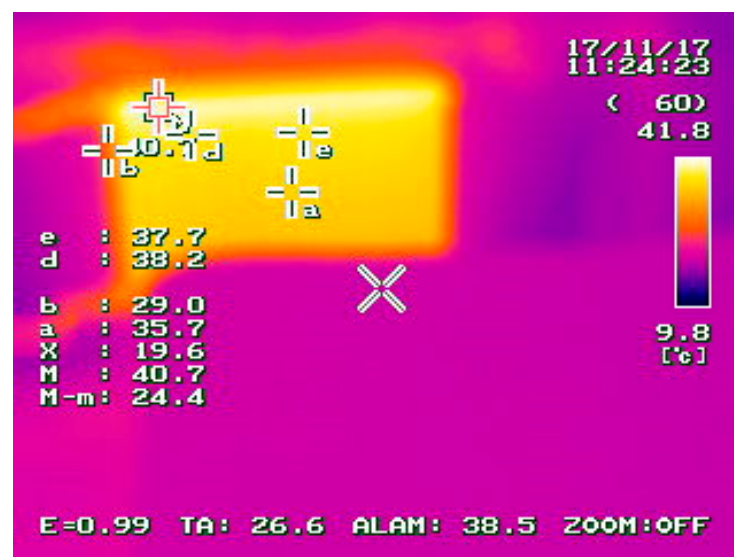


(a)



(b)

Figure 3. Cont.



(c)



(d)

**Figure 3.** A radiator of a SH system: (a,b), an old one, which is not even hot; (c,d), the same conditions and the same location but another room where a new radiator was installed. Note that although the maximum temperature is only 2.8 °C higher, it is the same for the whole radiator surface.

This results in lowering the temperature difference between the supply and return lines, which is an average of 16.5 °C. Hence, a larger amount of hot water inflows, although less heat per radiator is absorbed, much lower than regulated by the DH design guidelines to ensure 25 °C. This keeps the secondary return temperature high, consequently increasing the return temperature for a DH plant receiving return water from such a substation. This trend has been recorded in 31% of the inspected buildings. This results in the overheating of some spaces, the lowering of the indoor temperature (from the design one) in others, and also goes hand in hand with poor hydronic balancing being either a reason or a consequence. Even once a SH system is perfectly balanced, the return temperature after the substation may be still higher by 10–15%, and to address this issue, modernizing a substation is required. This could be also reasoned by consumers who install additional radiators to their SH systems to ensure comfort considerations. The issues reported by Kristensen et al. [4], such as ensuring warm feet on tiled bathroom floors by ordinary SH systems instead of maintaining the overall indoor temperature, are difficult to encounter in Russian cities such as Omsk or Krasnoyarsk.

To compare, Jangsten et al. [24] detected a trend of running at higher return temperature with an error of more than 1–2 °C, which is prescribed by the district cooling design guidelines. This behavior has been detected in 59% of the inspected buildings. The same was detected by Luc et al. [25], with the influence of internal heat gains also being visible for both new and old commercial buildings, where the temperature starts to increase after beginning a working day when the internal heat gains intensify. When looking at the graphs with the daily resolution, the same trend can be justified by considering the shortages of heat delivery due to the supply temperature being limited to 118 °C instead of the design upper threshold of 150 °C [30]. During these periods, the deviations are the largest ones (about 10–20 °C), while there is a threshold of outdoor temperature when the correct profile is achieved (about –15 °C). Thus, at –15 °C and above, no additional energy consumption is recorded. Once again, compared with Luc et al. [25], the increase in indoor temperature is caused by consumer's changes in the SH system such as changing radiators, installing or demounting electronic devices, and heat gains coming from electric heaters rather than from electronic device use and from occupants.

#### 4. Conclusions

Newer buildings have a lower but smoother profile of indoor temperature, whereas in older buildings, the indoor temperature might be unreasonably high, being 25–30 °C. The methodology suggests correction factors to enable a more thorough technical and economic review of a DH system. A better understanding of the system operation constitutes a necessary step in the process of switching to the 4GDH. An ordinary design approach results in the maximum possible demand of 299.7 kW. We suggest dumping heat with an indoor temperature of 20–25 °C by using the storage capacity of building envelopes, with no peak units (e.g., a heat pump) at all. Correcting a traditional approach when designing a building may minimize the energy consumption to 262.9 kW and increase the annual performance by up to 14.1%. The expected operation of both optimal designs (with the condition of optimal management of the substation) was analyzed with the help of the thermograms and modeling software. This means that the substation is assumed to be managed perfectly in line with design conditions, with no faulty equipment or any other operational issues such as increasing return temperature.

As suggested by the literature review, all the data-driven approaches agree on further tightening regulations of energy performance and a step-by-step conversion to 4GDH. Eventually, huge advantages may be achieved by the modernization of a conventional controller at a DH substation before two other primary steps (installing TES and running in low-temperature mode). The reductions in the thermal peak resulting from a new type of controller adjustment (for instance, discrete) compared to the traditional operation range from roughly 10 to 30%, respectively. This methodology simplifies all the implementations, accelerating the transition of district energy systems to new generations.

**Author Contributions:** Conceptualization, S.C. and A.Z.; methodology, S.C.; software, S.C.; validation, S.C., A.Z., and L.J.; formal analysis, S.C.; investigation, S.C.; resources, S.C.; data curation, S.C.; writing—original draft preparation, S.C.; writing—review and editing, S.C. and A.Z.; visualization, S.C.; supervision, A.Z.; project administration, A.Z.; funding acquisition, A.Z. All authors have read and agreed to the published version of the manuscript.

**Funding:** This research received no external funding.

**Institutional Review Board Statement:** Not applicable.

**Informed Consent Statement:** Not applicable.

**Data Availability Statement:** The data presented in this study are available on request from the corresponding author. The data is not publicly available due to confidentiality reasons.

**Conflicts of Interest:** The authors declare no conflict of interest.

## References

1. Fitó, J.; Hodencq, S.; Ramousse, J.; Wurtz, F.; Stutz, B.; Debray, F.; Vincent, B. Energy- and exergy-based optimal designs of a low-temperature industrial waste heat recovery system in district heating. *Energy Convers. Manag.* **2020**, *211*, 112753. [[CrossRef](#)]
2. Guelpa, E. Impact of thermal masses on the peak load in district heating systems. *Energy* **2021**, *214*, 118849. [[CrossRef](#)]
3. Turski, M.; Sekret, R. Buildings and a district heating network as thermal energy storages in the district heating system. *Energy Build.* **2018**, *179*, 49–56. [[CrossRef](#)]
4. Kristensen, M.H.; Hedegaard, R.E.; Petersen, S. Long-term forecasting of hourly district heating loads in urban areas using hierarchical archetype modeling. *Energy* **2020**, *201*, 117687. [[CrossRef](#)]
5. Brandi, S.; Piscitelli, M.S.; Martellacci, M.; Capozzoli, A. Deep reinforcement learning to optimise indoor temperature control and heating energy consumption in buildings. *Energy Build.* **2020**, *224*, 110225. [[CrossRef](#)]
6. Aryal, A.; Chaiwiwatworakul, P.; Chirattananon, S. An experimental study of thermal performance of the radiant ceiling cooling in office building in Thailand. *Energy Build.* **2023**, *283*, 112849. [[CrossRef](#)]
7. Vandermeulen, A.; van Oevelen, T.; van der Heijde, B.; Helsen, L. A simulation-based evaluation of substation models for network flexibility characterisation in district heating networks. *Energy* **2020**, *201*, 117650. [[CrossRef](#)]
8. Sun, C.; Chen, J.; Cao, S.; Gao, X.; Xia, G.; Qi, C.; Wu, X. A dynamic control strategy of district heating substations based on online prediction and indoor temperature feedback. *Energy* **2021**, *235*, 121228. [[CrossRef](#)]
9. Yuan, J.; Huang, K.; Han, Z.; Zhou, Z.; Lu, S. A new feedback predictive model for improving the operation efficiency of heating station based on indoor temperature. *Energy* **2021**, *222*, 119961. [[CrossRef](#)]
10. Sleptsov, A.; Crisostomi, E.; Bischì, A. Control schemes for district heating substations considering user-defined building's indoor temperature. *Build. Environ.* **2021**, *191*, 107598. [[CrossRef](#)]
11. Ivanko, D.; Sørensen, Å.L.; Nord, N. Splitting measurements of the total heat demand in a hotel into domestic hot water and space heating heat use. *Energy* **2021**, *219*, 119685. [[CrossRef](#)]
12. Chicherin, S.; Zhuikov, A.; Junussova, L. Integrating a heat pump into a 4th generation district heating (4GDH) system—Two-mode configuration inputting operational data. *Energy Build.* **2022**, *275*, 112445. [[CrossRef](#)]
13. Saletti, C.; Zimmerman, N.; Morini, M.; Kyprianidis, K.; Gambarotta, A. Enabling smart control by optimally managing the State of Charge of district heating networks. *Appl. Energy* **2020**, *283*, 116286. [[CrossRef](#)]
14. Braas, H.; Jordan, U.; Best, I.; Orozalieva, J.; Vajen, K. District heating load profiles for domestic hot water preparation with realistic simultaneity using DHWcalc and TRNSYS. *Energy* **2020**, *201*, 117552. [[CrossRef](#)]
15. Aste, N.; Caputo, P.; Del Pero, C.; Ferla, G.; Huerto-Cardenas, H.E.; Leonforte, F.; Miglioli, A. A renewable energy scenario for a new low carbon settlement in northern Italy: Biomass district heating coupled with heat pump and solar photovoltaic system. *Energy* **2020**, *206*, 118091. [[CrossRef](#)]
16. Sommer, T.; Sulzer, M.; Wetter, M.; Sotnikov, A.; Mennel, S.; Stettler, C. The reservoir network: A new network topology for district heating and cooling. *Energy* **2020**, *199*, 117418. [[CrossRef](#)]
17. Kauko, H.; Kvalsvik, K.H.; Rohde, D.; Nord, N.; Utne, Å. Dynamic modeling of local district heating grids with prosumers: A case study for Norway. *Energy* **2018**, *151*, 261–271. [[CrossRef](#)]
18. Hering, D.; Cansev, M.E.; Tamassia, E.; Xhonneux, A.; Müller, D. Temperature control of a low-temperature district heating network with Model Predictive Control and Mixed-Integer Quadratically Constrained Programming. *Energy* **2021**, *224*, 120140. [[CrossRef](#)]
19. Brange, L.; Englund, J.; Lauenburg, P. Prosumers in district heating networks—A Swedish case study. *Appl. Energy* **2016**, *164*, 492–500. [[CrossRef](#)]
20. Chertkov, M.; Novitsky, N.N. Thermal Transients in District Heating Systems. *Energy* **2019**, *184*, 22–33. [[CrossRef](#)]
21. Farouq, S.; Byttner, S.; Bouguelia, M.-R.; Nord, N.; Gadd, H. Large-scale monitoring of operationally diverse district heating substations: A reference-group based approach. *Eng. Appl. Artif. Intell.* **2020**, *90*, 103492. [[CrossRef](#)]
22. Chicherin, S.; Starikov, A.; Zhuikov, A. Justifying network reconstruction when switching to low temperature district heating. *Energy* **2022**, *248*, 123618. [[CrossRef](#)]
23. Siuta-Olcha, A.; Cholewa, T.; Gomółka, M.; Kołodziej, P.; Østergaard, D.S.; Svendsen, S. On the influence of decommissioning an area thermal substation in a district heating system on heat consumption and costs in buildings—Long term field research. *Sustain. Energy Technol. Assess.* **2022**, *50*, 101870. [[CrossRef](#)]
24. Jangsten, M.; Lindholm, T.; Dalenbäck, J.O. Analysis of operational data from a district cooling system and its connected buildings. *Energy* **2020**, *203*, 117844. [[CrossRef](#)]
25. Luc, K.M.; Li, R.; Xu, L.; Nielsen, T.R.; Hensen, J.L.M. Energy flexibility potential of a small district connected to a district heating system. *Energy Build.* **2020**, *225*, 110074. [[CrossRef](#)]
26. Harney, P.; Gartland, D.; Murphy, F. Determining the optimum low-temperature district heating network design for a secondary network supplying a low-energy-use apartment block in Ireland. *Energy* **2020**, *192*, 116595. [[CrossRef](#)]
27. Ren, C.; Cao, S.J. Construction of linear temperature model using non-dimensional heat exchange ratio: Towards fast prediction of indoor temperature and heating, ventilation and air conditioning systems control. *Energy Build.* **2021**, *251*, 111351. [[CrossRef](#)]
28. Camci, M.; Karakoyun, Y.; Acikgoz, O.; Dalkilic, A.S. A comparative study on convective heat transfer in indoor applications. *Energy Build.* **2021**, *242*, 110985. [[CrossRef](#)]

29. Johra, H.; Heiselberg, P.; Le Dréau, J. Influence of envelope, structural thermal mass and indoor content on the building heating energy flexibility. *Energy Build.* **2019**, *183*, 325–339. [[CrossRef](#)]
30. Chicherin, S.; Anvari-Moghaddam, A. Adjusting Heat Demands Using the Operational Data of District Heating Systems. *Energy* **2021**, *235*, 121368. [[CrossRef](#)]

**Disclaimer/Publisher's Note:** The statements, opinions and data contained in all publications are solely those of the individual author(s) and contributor(s) and not of MDPI and/or the editor(s). MDPI and/or the editor(s) disclaim responsibility for any injury to people or property resulting from any ideas, methods, instructions or products referred to in the content.